Analytical Biochemistry 428 (2012) 158–166

Contents lists available at SciVerse ScienceDirect

Analytical Biochemistry

journal homepage: www.elsevier.com/locate/yabio

Mammalian fatty acid synthase activity from crude tissue lysates tracing ^{13}C-labeled substrates using gas chromatography–mass spectrometry

Michael C. Rudolph [a,*], N. Karl Maluf [b], Elizabeth A. Wellberg [a], Chris A. Johnson [c], Robert C. Murphy [c], Steve M. Anderson [a]

[a] Department of Pathology, University of Colorado, Anschutz Medical Campus, Aurora, CO 80045, USA
[b] School of Pharmacy, University of Colorado, Anschutz Medical Campus, Aurora, CO 80045, USA
[c] Department of Pharmacology, University of Colorado, Anschutz Medical Campus, Aurora, CO 80045, USA

ARTICLE INFO

Article history:
Received 9 May 2012
Received in revised form 11 June 2012
Accepted 13 June 2012
Available online 20 June 2012

Keywords:
Fatty acid synthase
Gas chromatography–mass spectrometry
Mammary gland/liver lysates
^{13}C-labeled substrate incorporation
[$^{13}C_{16}$]palmitic acid

ABSTRACT

Fatty acid synthase (FASN or FAS, EC 2.3.1.85) is the sole mammalian enzyme to synthesize fatty acids de novo from acetyl- and malonyl-coenzyme A (CoA) esters. This article describes a new method that directly quantifies uniformly labeled $^{13}C_{16}$-labeled palmitate ([$^{13}C_{16}$]palmitate) by tracing [$^{13}C_2$]acetyl-CoA and [$^{13}C_3$]malonyl-CoA using an in vitro FASN assay. This method used gas chromatography–mass spectrometry (GC–MS) to detect [$^{13}C_{16}$]palmitate carboxylate anions (m/z 271) of pentafluorobenzyl (PFB) derivatives and was highly sensitive at femtomole quantities. Uniformly incorporated [$^{13}C_{16}$]palmitate was the primary product of both recombinant and crude tissue lysate FASN. Quantification of FASN protein within crude tissue lysates ensured equal FASN amounts, preserved steady-state kinetics, and enabled calculation of FASN-specific activity. FASN activity determined by [$^{13}C_{16}$]palmitate synthesis was consistent with values obtained from β-nicotinamide adenine dinucleotide 2′-phosphate (NADPH) oxidation assays. Analysis of FASN activity from tissue extracts was not hampered by contaminating enzymes or preexisting fatty acids. Crude mammary gland and liver lysates had significantly different activities at 82 and 65 nmol min^{-1} mg^{-1}, respectively, suggesting that tissue-specific activity levels differ in a manner unrelated to FASN amount. GC–MS quantification of [$^{13}C_{16}$]palmitate synthesis permits sensitive evaluation of FASN activity from tissues of varied physiological states and of purified FASN activity in the presence of modifying proteins, enzymes, or drugs.

Fatty acid synthase (FASN[1] or FAS, EC 2.3.1.85) is expressed in most human tissues and is indispensable in the mouse because the FASN null mice are embryonic lethal [1,2]. FASN is a complex enzyme that is absolutely essential for the cellular synthesis of short and medium chain fatty acids in mammals [3]. Mammalian FASN is an approximately 270-kDa enzyme that contains seven enzymatic domains and harbors the complete pathway to synthesize palmitic acid de novo from acetyl and malonyl esters of coenzyme A (CoA) as substrates (Fig. 1). The products of FASN, free fatty acids, have multiple biological functions, including lipid storage, phospholipid biosynthesis, both endocrine and nuclear hormone signaling ligands, and posttranslational modification of proteins [4–8]. FASN abundance and de novo fatty acid synthesis activity are commonly deregulated in a wide variety of human cancers and in metabolic diseases, underscoring the importance for the ability to study the enzyme [9–11]. Importantly, the enzymatic conversion of acetyl-CoA and malonyl-CoA substrates into palmitic acid can be recapitulated in the test tube, which has fostered elegant dissection of the mechanisms underlying FASN activity [3].

The majority of in vitro FASN activity assays can be grouped into two main categories: (i) assays that measure consumption/production of reaction components and (ii) assays that measure incorporation of heavy atom labeled substrates into the fatty acid products. Assays in the first group commonly quantify β-nicotinamide adenine dinucleotide 2′-phosphate (NADPH) oxidation into NADP$^+$ by monitoring changes in ultraviolet (UV) absorbance at 340 nm. Meticulous biochemistry during the 1990s determined the stereochemistry for the hydrogen atoms derived from NADPH, water, or malonyl-CoA during elongation of the fatty acyl chain to confirm that 14 molecules of NADPH are consumed for each palmitate synthesized [12,13]. Researchers have used this phenomenon

* Corresponding author. Fax: +1 303 724 3712.
E-mail address: michael.rudolph@ucdenver.edu (M.C. Rudolph).

[1] *Abbreviations used:* FASN (or FAS), fatty acid synthase; CoA, coenzyme A; PFB, pentafluorobenzyl; NADPH, β-nicotinamide adenine dinucleotide 2′-phosphate; CPM, 7-diethylamino-3-(4′-maleimidylphenyl)-4-methylcoumarin; GC–MS, gas chromatography–mass spectrometry; NICI, negative ion chemical ionization; DIEA, *N,N*-diisopropylethylamine; DTT, dithiothreitol; EDTA, ethylenediaminetetraacetic acid; DMSO, dimethyl sulfoxide; SDS, sodium dodecyl sulfate; PVDF, polyvinylidene fluoride; PFB-Br, pentafluorobenzyl bromine; MEC, mammary gland epithelial cell.

0003-2697/$ - see front matter © 2012 Elsevier Inc. All rights reserved.
http://dx.doi.org/10.1016/j.ab.2012.06.013

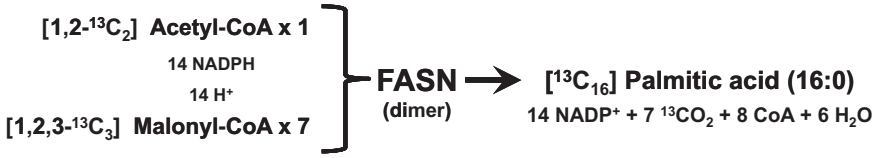

Fig.1. Reaction equation for the activity of fatty acid synthase showing conversion of [$^{13}C_2$]acetyl-CoA and [$^{13}C_3$]malonyl-CoA substrates, NADPH, and protons into 16-carbon saturated [$^{13}C_{16}$]palmitic acid plus by-products of enzyme catalysis.

to measure loss of absorption at 340 nm due to NADPH oxidation as a surrogate for FASN activity [14]. An alternative to evaluating NADPH consumption is to monitor the production of free CoA measured using fluorescent molecules that react with the free thiol of CoA such as 7-diethylamino-3-(4′-maleimidylphenyl)-4-methylcoumarin (CPM) [15,16]. However, free CoA plays a critical role in the initial substrate sorting steps of the FASN reaction, and as a result, scavenging of CoA using covalent dyes such as CPM could adversely affect FASN catalysis [17]. In addition to CoA scavenging, thiol-reactive dyes have the potential to bind to FASN, and this interaction could alter catalysis. Moreover, the use of thiol-reactive compounds to measure FASN activity in a crude tissue or cell lysate is likely to have decreased sensitivity due to dye interaction with molecules in the lysates. Despite these pitfalls, indirect assays for FASN activity remain popular and are used successfully largely because they use basic laboratory equipment, are easily scalable, and therefore are well suited for high-throughput screens.

FASN activity assays in the second category measure the end product of the FASN—de novo synthesized, nonesterified fatty acids. The majority of these assays rely on incorporation of a radioactive precursor into synthesized fatty acids and quantification of reaction products by liquid scintillation counting [18]. Others have used nonradioactive tracers, including D_2O and $^{13}C_1$-labeled malonyl-CoA ([$^{13}C_1$]malonyl-CoA) incorporation, to measure palmitate synthesis with success [19,20]. NADPH oxidation, radioactive tracers, and nonradioactive tracer methods have been problematic for a variety of reasons, including the indirect measurement of palmitate synthesis, loss of information about fatty acid chain length, hazardous radioactive waste, isotope purity of substrates, deuterium isotope effects, and decarboxylation of malonyl-CoA from crude tissue extracts. In this study, we describe a novel gas chromatography–mass spectrometry (GC–MS)-based FASN activity assay that uses high isotopic purity [$^{13}C_2$]acetyl-CoA and [$^{13}C_3$]malonyl-CoA reaction substrates to directly measure FASN product, de novo synthesized, uniformly incorporated [$^{13}C_{16}$]palmitate. This method is well suited for small-scale in vitro reactions with sensitivity at the femtomole level, uses commercially available 99% isotope purity substrates and standards, and calculates FASN-specific activity directly from crude extracts, obviating the need for complicated FASN purifications.

Materials and methods

GC–MS fatty acid quantification

Methods used in this study were adapted from Zarini and coworkers [21]. Sample analysis was performed by negative ion chemical ionization (NICI) GC–MS using the Finnigan DSQ GC–MS system (Thermo Finnigan, Thousand Oaks, CA, USA) with a ZB-l column (15 m–0.25 mm inner diameter, 0.10 mm film thickness, Phenomenex). The GC was programmed to increase the temperature from 125 to 230 °C at 20 °C/min, 230 to 245 °C at 5 °C/min, and finally 245 to 300 °C at 30 °C/min before being held at 310 °C for 1 min. The mass spectrometer was operated in the NICI mode using methane as reagent gas. Data were acquired in full scan mode to identify palmitic acid, [$^{13}C_{16}$]palmitate (m/z 271), and the internal standard [$^{13}C_4$]palmitate ion (m/z 259). Peak areas of the analyte or of the standard were measured, and the ratio of the area from the analyte-derived ion to that from the internal standard was calculated. The ratios were then compared with the calibration curve (see below) for the analyte prepared from commercially available standards to quantify [$^{13}C_{16}$]palmitate.

Palmitic acid calibration curve

[$^{13}C_{16}$]palmitate, [1,2,3,4-$^{13}C_4$]palmitate, and [D_{31}]palmitate were purchased from Sigma–Aldrich (St. Louis, MO, USA) with 99 atom% ^{13}C and 98 atom% D respectfully. Stock solutions for each compound were 1 mg/ml in 90% methanol. [$^{13}C_{16}$]palmitate was the analyte and [$^{13}C_4$]palmitate was the internal standard. The standard curve was prepared as a 5-fold serial dilution, and the analyte-to-standard ratios were measured in triplicate at seven different analyte amounts ranging from 460 pmol to 150 fmol, with the internal standard held constant at 8 pmol. Analyte-to-standard dilutions for generation of the standard curve made in 90% methanol were acidified to pH $\leqslant$ 4.0, isooctane extracted, derivatized, and transferred to vials as described in the next section, with the exception that the derivatized pellet for the 460-pmol point was resuspended in 1.0 ml of isooctane and that for the 150-fmol point was resuspended in 25 μl of isooctane.

Sample preparation for GC–MS

High-performance liquid chromatography (HPLC)-grade reagents were purchased from Sigma–Aldrich. Following the acidification step, 8 pmol of [$^{13}C_4$]palmitate was added as the internal reference standard, which locked the analyte-to-standard ratio prior to fatty acid extraction. Fatty acids were extracted with 1.0 ml of isooctane; samples were vortexed vigorously for 10 s and allowed to stand for 5 min at room temperature, after which they were centrifuged for 1 min at 300*g*. An 800-μl volume of the top organic phase was transferred to new glass tubes and taken to dryness using a Savant SpeedVac. Pellets were resuspended in 30 μl of 1% PFB bromide in acetonitrile, and 30 μl of 1% *N,N*-diisopropylethylamine (DIEA) dissolved in acetonitrile was added to initiate derivatization [21]. The derivatization reaction was allowed to proceed at room temperature for 30 min, after which the samples were dried using a Savant SpeedVac. The resulting pellets were resuspended in 100 μl (unless otherwise noted) of isooctane and transferred into vials for GC–MS.

FASN activity assay

Reactions were performed in a total volume of 200 μl, and FASN assay buffer consisted of 0.1 M potassium phosphate (pH 6.8), 1.0 mM dithiothreitol (DTT), and 1.0 mM ethylenediaminetetraacetic acid (EDTA). [1,2-$^{13}C_2$]acetyl-CoA at 99 atomic% ^{13}C, [1,2,3-$^{13}C_3$]malonyl-CoA at 99 atomic% ^{13}C, and NADPH reduced tetrasodium salt were purchased from Sigma–Aldrich. Reactions contained 2 μg (representing 36.7 nm dimer concentration) of recombinant FASN or FASN isolated from tissues (see below). Recombinant FASN or FASN isolated from tissues was diluted to 0.2 μg/μl in 250 mM potassium phosphate (pH

7.0), 1.0 mM DTT, and 1.0 mM EDTA and then equilibrated to room temperature for 1.0 h to restore FASN dimers. FASN assay buffer, 40 μM [$^{13}C_2$]acetyl-CoA, 180 μM NADPH, and 10 μl of diluted FASN (2 μg total) were preincubated at 37 °C for 2 min. The reactions were initiated by the addition of 110 μM [$^{13}C_3$]malonyl-CoA and mixed. Following a 60-s reaction time, the samples were quenched with 2 volumes (500 μl) of ice-cold methanol, acidified with 40 μl of 1.0 M HCl to approximately pH 3.5, and then gently vortexed. Cerulenin was purchased from Sigma–Aldrich and dissolved to 5 mM in dimethyl sulfoxide (DMSO). In experiments with cerulenin, samples were incubated in the FASN assay buffer without substrates for 30 min at room temperature, alone, with 6 μl of DMSO (2%, v/v) or with 1.0, 2.0, 10, 50, or 100 μM cerulenin (each in 6 μl of DMSO). Following cerulenin incubation, assay was conducted as before. Samples were then prepared for GC–MS as described above.

Recombinant FAS

Recombinant rat FASN enzyme was kindly provided by S. Smith and A. Witkowski (Children's Hospital Oakland Research Institute, Oakland, CA, USA). Enzyme concentration was measured using a Nanodrop spectrophotometer (Thermo Scientific), and concentration was estimated using a 280-nm extinction coefficient of 482,200 M^{-1} cm^{-1} (dimer without disulfides) according to Protein Calculator version 3.3 (http://www.scripps.edu/~cdputnam/protcalc.html) using rat FASN primary sequence at http://www.UniProt.org (entry P12785). Details of the preparation of C-terminally FLAG-tagged recombinant FASN can be found elsewhere [22]. Recombinant FASN protein was used to generate a standard curve to quantify the amount of FASN present in biological samples isolated from tissues. Triplicate dilutions ranging from 10 to 900 ng of FASN protein were run on sodium dodecyl sulfate (SDS) polyacrylamide gels, transferred to low-fluorescence polyvinylidene fluoride (PVDF) membrane (Millipore, Billerica, MA, USA), and incubated with 1:1000 FASN primary antibody from Santa Cruz Biotechnology (rabbit anti-human FASN, sc-20140, Santa Cruz, CA, USA), which was generated against a 299-amino acid region in the C terminus of human FASN (aa 2205–2504). The immunoblots were incubated in 1:15,000 goat anti-rabbit IRDye 800CW secondary (LI-COR Biosciences, Omaha, NE, USA). Infrared immunoblots were scanned using the LiCor Odyssey system, and data were analyzed using LiCor Image Studio 2.0 software (LI-COR Biosciences). Amounts of endogenous FASN were calculated according to the following equation:

$$\left(\text{Regression Slope in}\frac{\text{ng FASN}}{\text{Signal Intensity}}\right) \times \left(\frac{\text{Signal Intensity}}{60\ \mu\text{g Cytosolic Protien}}\right) = \frac{\text{ng FASN}}{\mu\text{g Cytosolic Protein}}$$

Isolation of FASN from mouse mammary gland and liver

Animals were maintained in the Center for Comparative Medicine under protocols approved by the institutional animal care and use committee of the University of Colorado–Denver. C57Bl/6 mice were purchased from Jackson Laboratories (Bar Harbor, ME, USA) and maintained on standard laboratory chow and a standard day/night cycle. Mammary gland epithelial cells were prepared as described previously with the exception that phenylmethanesulfonyl fluoride (PMSF) was omitted from the process [23]. Liver tissues from the identical mice used for preparation of mammary epithelial cells were collected and immediately snap-frozen on dry ice. Approximately 150 to 250 mg of tissue was homogenized in 1 ml of FASN lysis buffer (250 mM sucrose, 20 mM Hepes [pH 7.6], 2 mM $MgCl_2$, 1 mM DTT, 1 mM EDTA, 50 mM NaF, 5 mM $NaVO_4$, and 3× Roche complete EDTA-free protease inhibitors). Homogenized samples were centrifuged at 3500*g* for 10 min, and supernatant was collected and cleared at 100,000*g* for 30 min by ultracentrifugation. The protein concentrations present in the resulting cytosolic fraction were estimated using Pierce 660-nM Protein Assay (Thermo Fisher). A 60-μg amount of total cytosolic protein was loaded to denaturing SDS–PAGE (polyacrylamide gel electrophoresis) and transferred to low-fluorescence PVDF membrane (Millipore). Immunoblotting of FAS was performed as above using anti-FAS primary antibody and the Licor goat anti-rabbit IRDye 800cw secondary and was scanned using the LiCor Odyssey system. The amount of FASN present in tissue lysates was quantified by comparison with a standard curve using purified recombinant FASN. The volume of cytosolic extract representing 2 μg of FASN protein levels was evaluated using the FASN activity assay as above.

Results

GC–MS chromatograms and mass spectra of fatty acids

GC resolved individual PFB fatty acid esters of discrete chain lengths based on chromatography retention times. Pentafluorobenzyl bromine (PFB-Br) and DIEA were used as the derivatization agents that generated fatty acid carboxylate anions under NICI. The abundance of fatty acid carboxylate anions eluted from the column was detected by the mass spectrometer, which provided far superior signal-to-noise than other methods such as analysis of fatty acid methyl esters. Four palmitate isotopomers were purchased from a commercial vendor—unlabeled palmitate, [$^{13}C_4$]palmitate, [$^{13}C_{16}$]palmitate, and [D_{31}]palmitate—and an optimal internal reference standard was determined. These isotopomers of palmitic acid were mixed together, extracted, and derivatized, and then the mixture was subjected to GC–MS analysis. Identical retention times for unlabeled and ^{13}C-labeled palmitate are observed in the extracted ion chromatogram (Fig. 2A), but the retention time of the [D_{31}]palmitate (*m/z* 286) standard was shifted 8.4 s earlier. The unique *m/z* value of each palmitic acid isotopomer was readily distinguished by the mass spectrometer for the unlabeled palmitate (*m/z* 255), [$^{13}C_4$]palmitate (*m/z* 259), [$^{13}C_{16}$]palmitate (*m/z* 271), and [D_{31}]palmitate (*m/z* 286) carboxylate anions (Fig. 2B). Also detected were the carboxylate anions of the natural 1.1% abundance of ^{13}C of the isotopomers for unlabeled palmitate (*m/z* 256), [$^{13}C_4$]palmitate (*m/z* 260), and [D_{31}]palmitate (*m/z* 287). No natural 1.1% abundance of ^{13}C ion (e.g., *m/z* 272) was detected for [$^{13}C_{16}$]palmitate because all 16 carbons of palmitate were already ^{13}C labeled. Instead, a small fraction of [^{12}C]palmitate was detected (*m/z* 270) due to the 99 atom% ^{13}C isotopic purity from the commercial vendor. In addition, a large percentage of the [D_{31}]palmitate produced *m/z* 285, 284, and 283 ions, indicating that the 98 atom% D for this labeled palmitate was less than desirable. [$^{13}C_4$]palmitate was used as the internal standard and not [D_{31}]palmitate because the retention time was identical to [$^{13}C_{16}$]palmitate and [$^{13}C_4$]palmitate (*m/z* 259) differed by 12 Da from the [$^{13}C_{16}$]palmitate (*m/z* 271) synthesized in vitro by FASN.

A standard curve for quantification was established using [$^{13}C_{16}$]palmitate as the analyte and [$^{13}C_4$]palmitate as the internal standard. Six different amounts of [$^{13}C_{16}$]palmitate that spanned nearly four orders of magnitude (0.15–460 pmol) were subjected to GC–MS analysis. The signal ratio of the analyte to the standard relative to the amount of analyte generated a standard regression curve (Fig. 3A). The dilution series was conducted in triplicate and had an R^2 correlation value of 0.9991 with a slope of 0.104 ± 0.00007, and the inset of Fig. 3A shows linearity of the low end of the curve (0.15–3.7 pmol of analyte). This method was highly sensitive and

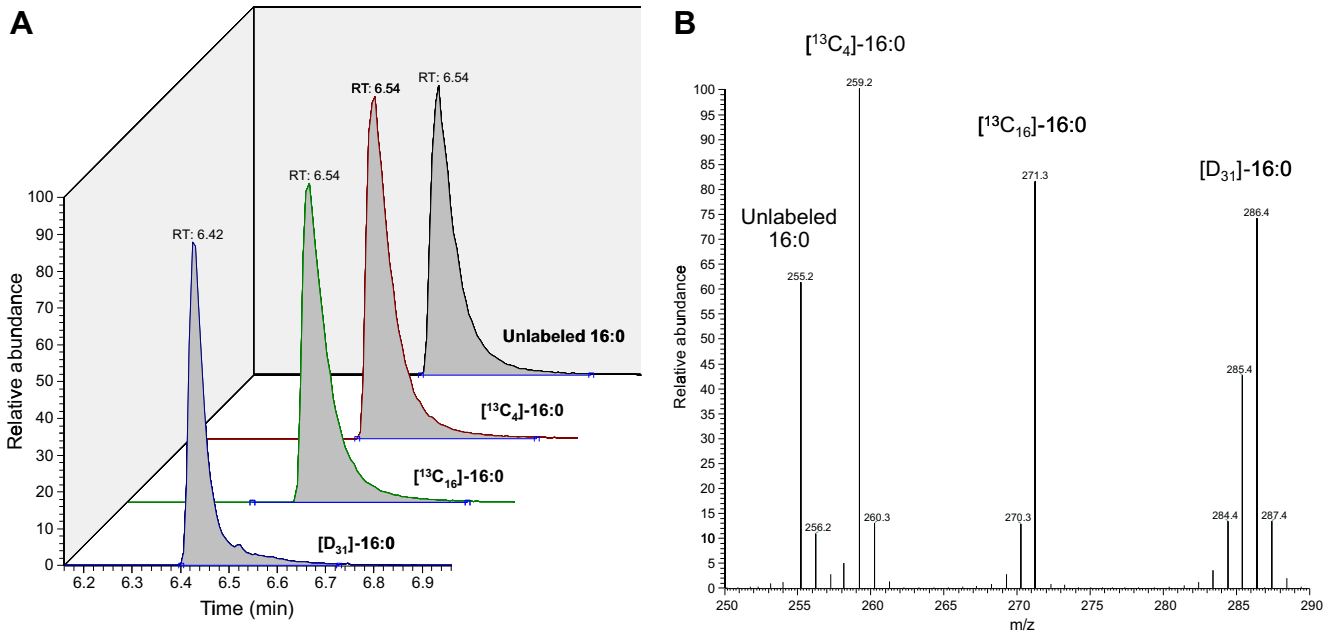

Fig.2. Extracted ion chromatogram and spectrum of commercially available isotopomers of palmitate (16:0) mixed together, extracted, derivatized, and injected into the GC–MS. (A) Resolution of PFB fatty acid esters by chromatographic retention time. [$^{13}C_4$]palmitate and [$^{13}C_{16}$]palmitate coeluted at 6.54 min with the unlabeled palmitate, but [D_{31}]palmitate eluted from the column 0.14 min (8.4 s) earlier than the [^{13}C]palmitate molecules. (B) Extracted ion spectrum from retention time 6.40 to 6.7 for carboxylate anions of palmitate isotopomers at *m/z* 255 (unlabeled), *m/z* 259 ($^{13}C_4$), *m/z* 271 ($^{13}C_{16}$), and *m/z* 286 (D_{31}).

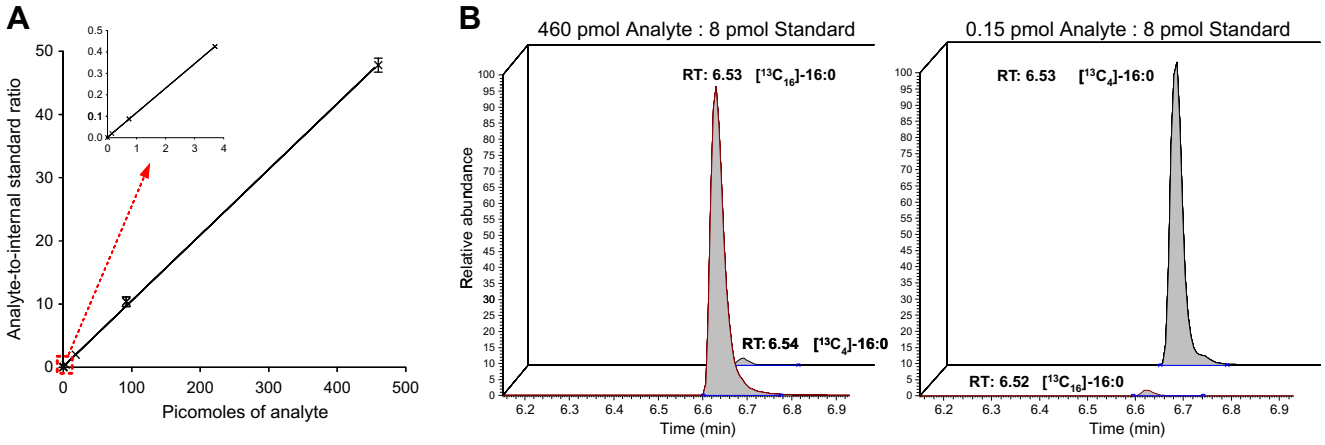

Fig.3. (A) Serial dilution regression curve of the [$^{13}C_{16}$]palmitate analyte-to-[$^{13}C_4$]palmitate standard ratio relative to the amount of analyte. The analyte amount varied from 0.15 to 460 pmol, and the standard was held at 8 pmol. The dilution series was performed in triplicate, with a slope of 0.104 and a correlation value of 0.9991. The inset shows the range from 0.15 to 3.7 pmol of analyte. B) Extracted ion chromatograms for the 460:8 pmol point (left) and the 0.15:8 pmol point (right) for the [$^{13}C_{16}$]palmitate analyte (front peaks) and the [$^{13}C_4$]palmitate standard (back peaks). The sensitivity of this assay was 0.15 pmol of [$^{13}C_{16}$]palmitate analyte.

routinely capable of detecting [$^{13}C_{16}$]palmitate fatty acid carboxylate anions at and below 150 fmol. The relative abundance of the 460 pmol and 150 fmol [$^{13}C_{16}$]palmitate analyte (front peaks) to the internal [$^{13}C_4$]palmitate 8-pmol standard (back peaks) is demonstrated in the extracted ion chromatograms (Figs. 3A and B). The strong linear correlation value of the standard curve, combined with the sensitivity of the mass spectrometer using PFB fatty acid derivatives, enabled measurements with a broad dynamic range down to femtomole amounts of [$^{13}C_{16}$]palmitate.

FASN activity assay

Conditions of the in vitro assay were established using affinity-purified recombinant rat FASN isolated from Sf9 insect cells infected with the full-length FASN-encoding baculovirus expression vector. FASN activity assays have been well defined in the literature [18,24] and were conducted with minor modifications according to Materials and Methods. FASN dimerization is required for complete enzyme activation and subsequent synthesis of palmitic acid, but dimer assembly is sensitive to temperatures below 20 °C and solutions of low ionic strength (<50 mM potassium phosphate buffer), such that FASN dimers slowly dissociate under either condition [25]. A critical aspect of either the [$^{13}C_{16}$]palmitate synthesis or NADPH oxidation method for FASN activity was fully assembled FASN dimers. Recombinant FASN or tissue-derived FASN was routinely incubated in 0.25 M potassium phosphate (pH 7.0), 1 mM EDTA, 1 mM DTT, and 10% glycerol for 1 h at room temperature to facilitate FASN dimer assembly. Without this process, only 20% of

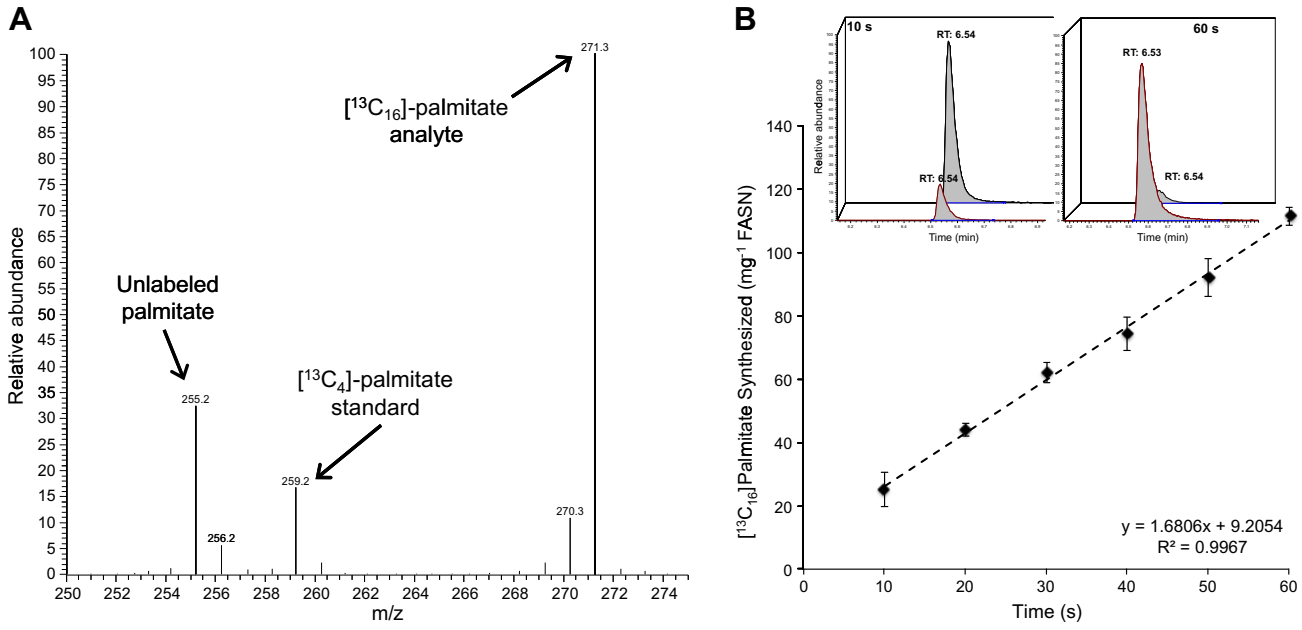

Fig.4. (A) Extracted ion spectrum for [$^{13}C_{16}$]palmitate analyte (*m*/*z* 271), [$^{13}C_4$]palmitate (*m*/*z* 259) standard, and unlabeled palmitate (*m*/*z* 255) from the recombinant FASN assay. The primary product is [$^{13}C_{16}$]palmitate when supplying [$^{13}C_2$]acetyl-CoA and [$^{13}C_3$]malonyl-CoA substrates in the reaction. (B) Recombinant FASN activity over 1 min monitoring the [$^{13}C_{16}$]palmitate carboxylate anion (*m*/*z* 271). The reaction proceeds linearly, demonstrating steady-state kinetics and that recombinant FASN synthesized 101 nmol [$^{13}C_{16}$]palmitate min^{-1} mg^{-1}. The abundance of [$^{13}C_{16}$]palmitate (front peak) relative to the [$^{13}C_4$]palmitate standard (back peak) in extracted ion chromatograms for the 10- and 60-s points increased over time (insets).

the fully reactivated FASN activity was observed (data not shown). The need to reactivate recombinant, purified, or crude tissue lysate FASN was underscored by the observation that FASN reactivation (dimer assembly) occurred during the reaction at 37 °C because the rate of [$^{13}C_{16}$]palmitate synthesis was parabolic up to 2 min into the reaction when the rate then became linear (not shown).

The primary product of recombinant FASN was [$^{13}C_{16}$]palmitate (*m*/*z* 271) when the reaction was supplied with [$^{13}C_2$]acetyl-CoA and [$^{13}C_3$]malonyl-CoA substrates (Fig. 4A). The ion *m*/*z* 270 [$^{13}C_{16}$]palmitate was also routinely detected, which was due to the 99 atomic% ^{13}C of the two substrates. Also detected in the FASN activity assay was unlabeled palmitate (*m*/*z* 255) that originated from the stock of purified recombinant enzyme. The presence of *m*/*z* 255 unlabeled palmitate ion was verified by extracting fatty acids from the recombinant enzyme stock alone (data not shown). Here, 50-μl volumes were sampled every 10 s for 60 s, and the reaction proceeded linearly and under steady-state kinetics (Fig. 4B). Working reaction conditions were determined for optimal steady-state kinetics of FASN by varying substrate concentrations over a longer time series, and the best time frame and substrate concentrations that yielded the most optimal slope and linearity (R^2 correlation value) were selected. Later time points, such as 90 and 120 s, using 40 μM [$^{13}C_2$]acetyl-CoA and 110 μM [$^{13}C_3$]malonyl-CoA tended to plateau, indicating that the reaction had deviated from steady-state kinetics, presumably due to high concentrations of free CoA that inhibits FASN catalysis [17]. The amount of [$^{13}C_{16}$]palmitate synthesized in the reaction was quantified relative to the analyte-to-standard ratio regression curve (Fig. 3). FASN synthesized [$^{13}C_{16}$]palmitate at 101 nmol min^{-1} mg^{-1} (Fig. 4B), and the increased *m*/*z* 271 [$^{13}C_{16}$]palmitate (front peak) relative to *m*/*z* 259 [$^{13}C_4$]palmitate standard (back peak) from 10 to 60 s (left and right insets of Fig. 4B, respectively) is represented in extracted ion chromatograms. The NADPH oxidation method was then compared with the direct quantification of [$^{13}C_{16}$]palmitate (Table 1). NADPH oxidation was monitored continuously via the spectrophotometric method and FASN oxidized overall 1544 nmol NADPH min^{-1} mg^{-1} (±137) compared with the [$^{13}C_{16}$]palmitate at 102 nmol min^{-1} mg^{-1} (±4.9) synthesized by FASN in that set of experiments. Because 14 molecules of NADPH are oxidized per molecule of [$^{13}C_{16}$]palmitate synthesized, 102×14 gives a converted NADPH oxidation of

Table 1
Comparison of NADPH oxidation with direct [^{13}C]$_{16}$-palmitate quantification.

	Sample 1	Sample 2	Sample 3	Sample 4	Average
NADPH run 1	1267.2	1459.2	1546.0	1612.8	1469 (±77)
NADPH run 2	1632.0	1536.0	1728.0	1584.0	1616 (±100)
Overall average	1544 (±137)				
Converted	110.0				
[$^{13}C_{16}$]palmitate 1	98.4	101.4	96.8	109.4	101 (±5.6)
[$^{13}C_{16}$]palmitate 2	108.8	98.5	105.2	100.2	103 (±5.22)
Overall average	102 (±4.9)				

Note. The [$^{13}C_{16}$]palmitate quantification method was compared with the NADPH oxidation method using recombinant FASN and identical reaction conditions outlined in Materials and Methods. Oxidation of NADPH was continuously monitored on two different runs, and numbers are expressed as nmoles NADPH oxidized min^{-1} mg^{-1}. In two separate experiments, the [$^{13}C_{16}$]palmitate carboxylate anion (*m*/*z* 271) was monitored and quantified relative to the regression curve in Fig. 3. Specific activity of recombinant FASN using the NADPH method was 1544 nmol min^{-1} mg^{-1}, and FASN synthesized [$^{13}C_{16}$]palmitate at 102 nmol min^{-1} mg^{-1}. NADPH oxidation was converted to nmoles palmitate by dividing 1544 by 14, which gave 110 nmol min^{-1} mg^{-1}, because 14 molecules of NADPH are oxidized during the synthesis of one palmitate molecule.

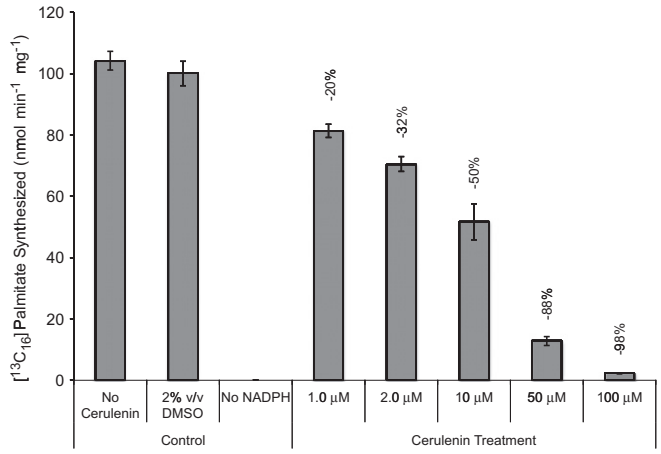

Fig.5. Recombinant FASN activity assay performed according to conditions in Materials and Methods. Samples were incubated with and without increasing concentrations of cerulenin. The [$^{13}C_{16}$]palmitate carboxylate anion *m*/*z* 271 was monitored and quantified relative to the regression curve in Fig. 3A. Specific activity of recombinant FASN without cerulenin synthesized [$^{13}C_{16}$]palmitate at 104 nmol min^{-1} mg^{-1} and [$^{13}C_{16}$]palmitate synthesis was significantly inhibited by 20% ($P = 0.0018$) with 1 µM cerulenin up to 98% with 100 µM cerulenin (32–98% samples, $P \leqslant 0.0005$). DMSO (2%, v/v) had no effect on the reaction, and the [$^{13}C_{16}$]palmitate carboxylate anion *m*/*z* 271 was not detected in the absence of NADPH.

1428 nmol min^{-1} mg^{-1}. Thus, the two methods differ by 7.5% and are in reasonable agreement when measuring the activity of recombinant FASN.

PFB derivatives of [$^{13}C_{16}$]palmitate from commercial sources generated a carboxylate anion at *m*/*z* 271. Spectra from commercial [$^{13}C_{16}$]palmitate compared with spectra from recombinant FASN validated that [$^{13}C_{16}$]palmitate was a direct product of FASN catalysis. In addition, exclusion of NADPH from the reaction resulted in no *m*/*z* 271 carboxylate anion from [$^{13}C_{16}$]palmitate; therefore, no FASN catalysis occurred (Fig. 5). [$^{13}C_{16}$]palmitate synthesis was evaluated in the presence of the "suicide" FASN inhibitor cerulenin. Cerulenin is known to irreversibly inhibit the β-ketoacyl synthase condensing enzyme domain of type I fatty acid synthases, and inhibitory concentrations are known to be directly proportional to FAS inhibition [26,27]. The addition of DMSO (2%, v/v), the solvent for cerulenin, did not alter the synthesis of [$^{13}C_{16}$]palmitate, and nearly the same reaction rate was observed compared with no cerulenin (Fig. 5). Cerulenin was added at various concentrations to reactions, and reactions were carried out according to Materials and Methods. [$^{13}C_{16}$]palmitate synthesis was inhibited by 20% ($P = 0.0018$) with 1 µM cerulenin and suppressed 88% by the addition of 50 µM cerulenin at 12.8 (±1.5) nmol min^{-1} mg^{-1} relative to no cerulenin conditions at 104 nmol min^{-1} mg^{-1} (Fig. 5). The addition of 100 µM cerulenin resulted in near complete (98%) inhibition of [$^{13}C_{16}$]palmitate synthesis (32–98% samples, $P \leqslant 0.0005$). By using ^{13}C-labeled acetyl-CoA and malonyl-CoA incorporation to directly measure [$^{13}C_{16}$]palmitate synthesis, this method was capable of investigating enzyme inhibition in vitro with enough sensitivity to detect very subtle changes in catalysis at lower than reported drug concentrations. A significant 20% inhibition was observed ($P = 0.0018$) at 1.0 µM cerulenin. These data demonstrate a specific and sensitive method to directly quantify FASN catalyzed synthesis of [$^{13}C_{16}$]palmitate.

FASN activity assay from tissue extracts

Of great interest is to evaluate the FASN activity directly from crude lysates of a wide variety of tissues and cell lines under normal and pathological conditions. A critical aspect when using crude cell or tissue extracts is the amount of "contaminating enzymes" within the cytosolic fraction [28]. Contaminating enzyme activity was generally avoided using complicated FASN purification methods such as anion exchange chromatography [29]. Added to the difficulty of evaluating FASN activity from crude lysates was that FASN protein amounts could not be quantified. Calculation of FASN amount from crude lysates is necessary for several reasons: to ensure that the amount of enzyme from each sample is equivalent, to be certain that the levels of FASN in the in vitro assay preserve steady-state kinetics, and to calculate the specific activity based on milligrams of FASN. Crude cytosolic lysate FASN from mammary gland and liver tissues was quantified using an immunoblot approach relative to a standard regression curve generated with recombinant rat FASN (Fig. 6A). The anti-FASN antibody is a rabbit polyclonal generated against a 299-amino acid region (aa 2205–2504) at the C terminus of human FASN. There is 95% sequence identity (283/299 amino acids) between human and mouse FASN in this region, 94% identity (280/299 amino acids) between human and rat FASN in this region, and 97% identity (296/304 amino acids) between rat and mouse FASN, suggesting that the cross-reactivity between rat and mouse epitopes is robust. Immunoblots were quantified using the Licor Odyssey instrument, and each standard

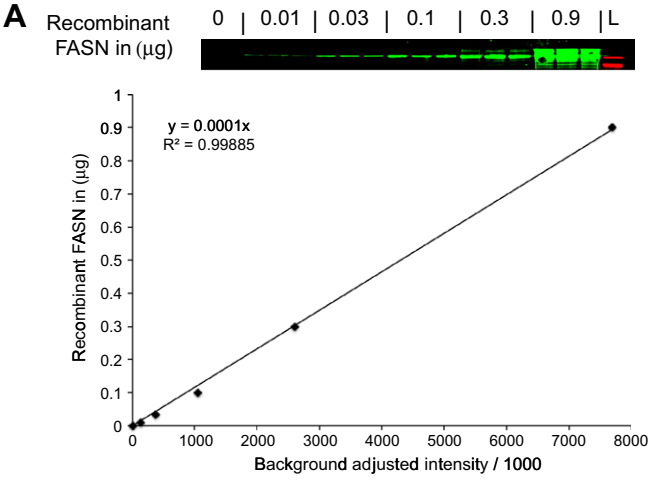

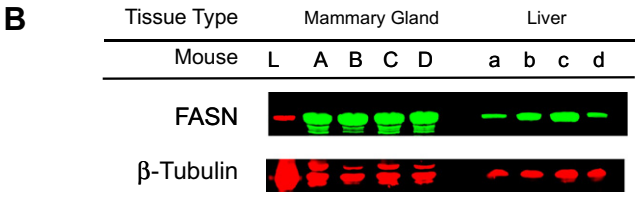

Mouse	FAS in ng/µg cytosolic extract	
A	37.7	13.6
B	41.4	21.8
C	37.2	32.9
D	38.3	11.3
Mean (SEM)	38.6 (+/- 1.9)	19.8 (+/- 9.7)

Fig.6. (A) Regression curve for the serial dilution series using known amounts of recombinant FASN protein (in µg). The dilution was performed in triplicate with a correlation value of 0.99885. The slope of the dilution series was used to calculate the amount of FASN isolated from tissue extracts. (B) Calculation of FASN quantity (in ng/µg) of cytosolic extract from mammary gland epithelium and from liver tissues. Values in the table are calculated from the signal intensity values quantified in the immunoblot for all immunoreactive bands shown. These signal intensity values are relative to the recombinant FASN regression curve in panel A and are calculated according to the equation in Materials and Methods. L denotes the marker ladder for the immunoblot.

curve dilution point was evaluated in triplicate. A regression line was generated with a slope of 0.0001 and an R^2 correlation value of 0.99885. Next, crude cytosolic fractions were prepared from mammary gland epithelial cells (MECs), and matched livers of the same animals as described in Materials and Methods and amounts of crude cytosolic lysate FASN were calculated using the recombinant FASN regression curve. When standardized to 60 μg of total cytosolic fraction protein, crude lysate FASN was quantified using the signal intensity values from all immunoreactive bands shown (Fig. 6B). FASN amounts were consistent from the MECs but variable from the liver. β-Tubulin indicated cytosolic protein in each well but was not used for any quantification or normalization purposes. Crude lysate FASN from MECs and liver FASN was estimated at 38.6 (±1.9) and 19.8 (±9.7) ng/μg cytosolic protein, respectively. Using this strategy to quantify endogenous FASN in each sample (table in Fig. 6B), a known FASN amount was added to the following activity assays.

FASN from crude cytosolic extracts of both tissues synthesized [$^{13}C_{16}$]palmitate (*m*/*z* 271) as the primary reaction product (Fig. 7). A large quantity of preexisting unlabeled palmitate derived from the cytosolic fractions of the lysates was detected (*m*/*z* 255 ion, shown), as were unsaturated fatty acids 18:1 *m*/*z* 281 and 18:2 *m*/*z* 279 that did not originate from FASN catalysis in the assay (data not shown). Detection of preexisting fatty acids in the lysates emphasized the importance of supplying uniformly ^{13}C-labeled substrates in the crude FASN assay reaction because variable levels of unlabeled palmitate would confound palmitate detection using unlabeled substrates. The ion *m*/*z* 270 resulted from the 99 atom% ^{13}C isotopic purity of the substrates, as was observed from the recombinant FASN assays. The specific activity of FASN from the crude cytosolic MECs and the liver lysates was calculated (Fig. 7B). Equalized amounts (2 μg) of MECs and liver FASN synthesized [$^{13}C_{16}$]palmitate at 82 and 65 nmol min^{-1} mg^{-1} FASN, respectively. The specific activity of FASN from in vivo samples was 20 to 35% less than that observed for recombinant FASN. Although the amount of FASN from the crude cytosolic extracts was equal, the mammary gland FASN had significantly higher specific activity (1.26-fold, $P = 0.02$) compared with liver FASN, a trend that was observed in three independent experiments. This observation suggested that the 1.26-fold difference might be due to factors other than overall enzyme abundance. Finally, the addition of 100 μM cerulenin inhibited FASN catalysis by more than 93% (Fig. 7B), which validated that the presence of the [$^{13}C_{16}$]palmitate *m*/*z* 271 carboxylate anion in reaction using crude lysates was due to FASN.

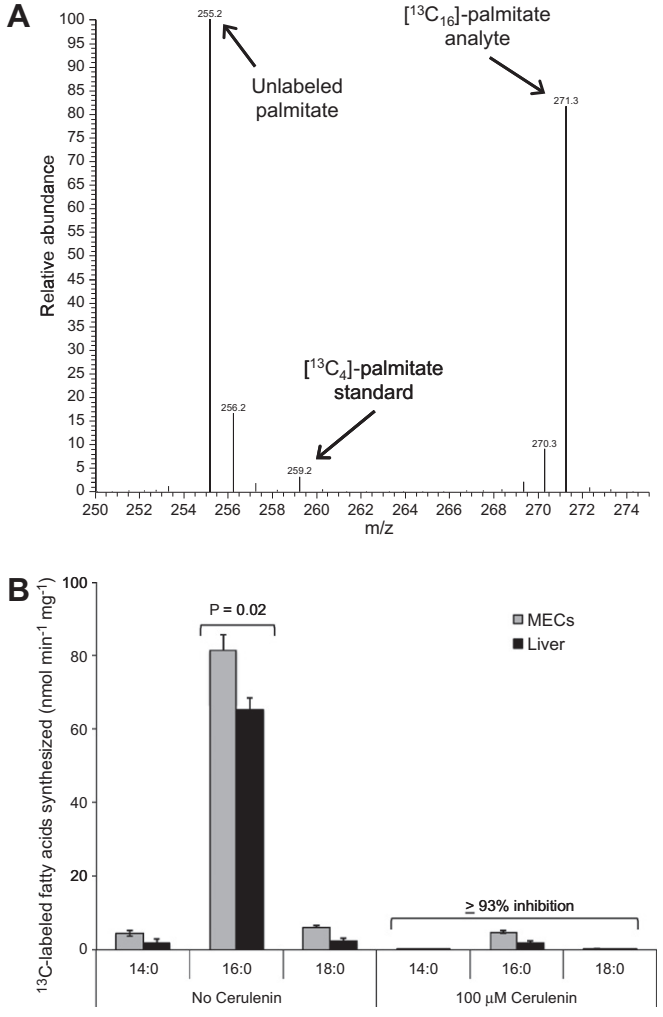

Fig.7. (A) Extracted ion spectrum of the FASN activity assay using tissue-derived FASN. The primary reaction product is uniformly incorporated [$^{13}C_{16}$]palmitate (*m*/*z* 271). Unlabeled palmitate (*m*/*z* 255) was detected in the spectrum from the crude cytosolic extract, and [$^{13}C_4$]palmitate (*m*/*z* 259) is the internal standard. (B) FASN activity assay using the volume of crude cytosolic extracts that corresponded to 2 μg of total FASN from mammary epithelial cells and livers of the same mice. A 1.26-fold ($P = 0.02$) significant decrease in specific activity was observed by liver FASN for [$^{13}C_{16}$]palmitate synthesis. Reactions were conducted according to Materials and Methods without and with 100 μM cerulenin, inhibiting FASN activity greater than 93%. Data plotted were quantified by monitoring [$^{13}C_{14}$]myristate (*m*/*z* 241), [$^{13}C_{16}$]palmitate (*m*/*z* 271), and [$^{13}C_{18}$]stearate (*m*/*z* 301) ions.

Discussion

FASN has been studied by biochemists for decades to elucidate enzyme mechanism and reaction kinetics and to determine the requirements for enzyme catalysis. Here, a new method to directly quantify [$^{13}C_{16}$]palmitate synthesis that uses the incorporation of high-purity, nonradioactive heavy atom [$^{13}C_2$]acetyl-CoA and [$^{13}C_3$]malonyl-CoA substrates has been described (Fig. 1). This method detected carboxylate anions of [$^{13}C_{16}$]palmitate PFB derivatives using GC–MS. GC–MS simultaneously measured both the [$^{13}C_{16}$]palmitate analyte and the [$^{13}C_4$]palmitate internal standard at the same retention time to provide greater precision than noninternal standards [30]. The finding that the primary product of FASN is saturated palmitate was validated using this method by comparing the *m*/*z* 271 ion of [$^{13}C_{16}$]palmitate with purchased [$^{13}C_{16}$]palmitate. GC–MS directly quantifies de novo fatty acid synthesis in vitro, and the specific activity for both recombinant FASN and tissue-derived FASN was determined. This new method integrates the use of [$^{13}C_2$]acetyl-CoA and [$^{13}C_3$]malonyl-CoA heavy atom tracers with the power of GC–MS to provide a very sensitive assay that detects FASN catalyzed de novo synthesized fatty acids at the femtomole level. Most important, this method is not confounded by the presence of unlabeled palmitate that often contaminates solvents and blanks because it measures [$^{13}C_{16}$]palmitate synthesis from uniformly ^{13}C-labeled acetyl- and malonyl-CoA esters.

The direct quantification of [$^{13}C_{16}$]palmitate was compared with the NADPH oxidation method using recombinant FASN and identical reaction conditions according to Materials and Methods. The values observed in Table 1 are consistent with previous reports of FASN activity calculated using the NADPH oxidation method that indicated a broad range of values between 1500 and 2000 nmol min^{-1} mg^{-1} [24,29,31,32]. In our hands, the NADPH oxidation method gave 1544 nmol min^{-1} mg^{-1}. The direct [$^{13}C_{16}$]palmitate quantification method was consistent with, but slightly lower than, reported results at approximately 1428 nmol NADPH oxidized min^{-1} mg^{-1} (converted by multiplying 102 nmol min^{-1} mg^{-1} times 14). The [$^{13}C_{16}$]palmitate quantification value is slightly lower, presumably because we monitored the abundance of only the [$^{13}C_{16}$]palmitate carboxylate anion at *m*/*z* 271. To that end, other FASN products are synthesized in the

reaction, including myristic and stearic acids and short acyl "by-products" of FASN such as butyryl (4:0) and crotonyl (4:1) CoA esters [33]. With respect to palmitate synthesis, these additional FASN products all consume NADPH over the course of the reaction. Because oxidation of NADPH was used to calculate FASN catalysis, the production of these minor products alters calculations of FASN activity from NADPH oxidation during continuous 340-nM monitoring of the aqueous reaction mixture using the spectrophotometric method. This observation suggested that the difference in calculation of specific activity could be a result of the methods used rather than due to variations in catalysis of recombinant FASN itself.

Previous methods to quantify fatty acids typically used radioactive materials and liquid scintillation counting to measure fatty acid synthesis. Although this procedure successfully measures the products of FASN catalysis, critical information regarding fatty acid chain length cannot be determined using this approach. Conventional GC is useful to discriminate among fatty acids of varied chain length [4]; however, heavy atom tracer information would be lost using standard flame ionization. Radiolabeled GC was used to quantify fatty acids of various chain lengths by retention time, and it retains radioactive tracer content; however, quantification of each fatty acid is accomplished using reference standards that are unrelated to the fatty acid of interest [34,35]. Radiolabeled HPLC methods also exist to resolve and detect discrete fatty acid chain lengths using flow-through scintillation detectors [33,36]. Although the sensitivity of radioassays is quite good, the accuracy is often poor [20]. Both liquid scintillation counting and radio chromatography techniques use radioactive materials that are often expensive, require special handling, and cause difficulty for waste disposal due to the generation of hazardous mixed wastes. This method directly quantified FASN activity using [$^{13}C_2$]acetyl-CoA and [$^{13}C_3$]malonyl-CoA incorporation to avoid the undesirable issues with radioisotope methods.

Two methods were reported for either deuterium or [$^{13}C_1$]malonyl-CoA incorporation into labeled palmitate using a similar in vitro FASN activity assay and GC–MS [19,20]. Monitoring deuterium incorporation was not desirable due to isotope effects of deuterium in the FASN assay [13,19]. Alternatively, Ohashi and coworkers compared the NADPH method with [$^{13}C_1$]malonyl-CoA incorporation into ^{13}C-labeled de novo fatty acids synthesized by column-purified FASN and FASN from crude cytosolic extracts [20]. A major issue with this study was the isotopic purity of the [$^{13}C_1$]malonyl-CoA used in the FASN assay; [$^{13}C_1$]malonyl-CoA was synthesized and purified in the lab at 92 atom% ^{13}C isotopic purity with the label at the central methylene carbon of malonyl-CoA. Using lower purity [$^{13}C_1$]malonyl-CoA, Ohashi and coworkers detected $^{13}C_6$-, $^{13}C_7$-, and $^{13}C_8$-incorporated palmitate requiring summation of these ions [20]. Conversely, commercial sources currently exist to provide 99 atom% ^{13}C isotopic purity of [$^{13}C_2$]acetyl-CoA and [$^{13}C_3$]malonyl-CoA substrates, which enables synthesis of completely incorporated [$^{13}C_{16}$]palmitate (m/z 271) and only minor amounts of the [$^{13}C_{16}$]palmitate carboxylate anion (m/z 270) ($\leqslant$10%). Another improvement from the method reported by Ohashi and coworkers, who measured fatty acid methyl esters and McLafferty rearrangement ion m/z 74, is the quantitation of carboxylate anions of nonfragmented fatty acids [20]. PFB-Br/DIEA derivatization of [$^{13}C_{16}$]palmitate generated carboxylate anions of fatty acids that were robustly detected by the mass spectrometer, resulting in an excellent signal-to-noise ratio. The derivatization strategy for this method was sensitive in the low femtomole range, which was far superior to either the NADPH oxidation method or the quantitation of fatty acid methyl esters. Finally, the previous [$^{13}C_1$]malonyl-CoA used nanomolar concentrations of substrates over a 30-min reaction, which did not measure fatty acid synthesis reaction under steady-state conditions from either column-purified FASN or crude extracts.

Researchers have routinely isolated FASN from mammary tissues and liver, and some have purified FASN from tumors and tumor cell lines to investigate enzyme activity [18,37,38]. However, calculating FASN concentrations from crude lysates of biological samples has been difficult. The addition of known FASN amounts to the reaction is essential to ensure that the analysis is conducted under steady-state conditions. Here, we have described an immunoblotting approach to calculate the amount of FASN, eliminating the need for enzyme purification that typically abolishes protein–protein interactions that may be important in understanding the cell-type specific biology. To that end, crude tissue lysates are known to contain "interfering enzymes" that could consume NADPH or decarboxylate malonyl-CoA or could alter acetyl-CoA levels [20,28,39]. For example, the presence of interfering enzymes might affect calculations of FASN activity via NADPH oxidation if NADPH is oxidized by factors other than FASN. In addition, decarboxylation of malonyl-CoA by malonyl-CoA decarboxylase in the crude lysate results in acetyl-CoA, which would alter the levels of malonyl-CoA that are needed for acyl elongation by FASN. Conversely, this method supplied micromolar concentrations of [$^{13}C_2$]acetyl-CoA, [$^{13}C_3$]malonyl-CoA, and NADPH, which insulated FASN catalysis against interfering enzymes present in crude lysates. Therefore, the method outlined is suitable to conduct FASN assays using tissue-derived crude cytosolic fractions.

FASN protein from crude in vivo extracts was quantified to enable calculation of the specific activity based on milligrams of FASN added to the reaction. The mammary gland samples contained several minor bands detected in the immunoblot but not present in the liver samples. It is not clear whether these minor products represent a catalytically functional FASN or if they are breakdown products of nonfunctional FASN. The specific activity of FASN from the crude extracts was 20% to 35% less than that observed for recombinant FASN. It is possible that the immunoblotting approach used to quantify mouse FASN in crude cytosolic extracts, relative to a rat FASN regression curve, introduced error into the calculation of specific activity for the mouse enzyme. However, the epitope of the anti-FASN antibody for mouse and rat was highly similar (97% identical) and is unlikely to account for the 20 to 35% difference in activity. This means that the trend observed between mouse tissue extracts would not be altered, even though the "absolute" amount of total FASN could be variable. The difference between mouse crude extract FASN and the affinity-purified rat FASN could be species specific; however, column-purified FASN from species as divergent as rat and chicken had nearly identical activities at 1500 to 2000 and 1600 nmol NADPH oxidized min^{-1} mg^{-1}, respectively [24,29]. On the other hand, the 20% to 35% difference was consistent with the observations that compared recombinant FASN with tissue-derived FASN, where the tissue-derived FASN had lower activity than the purified recombinant FASN [29]. We speculate that the difference in activity between the mouse and the rat synthases is most likely due to the type of FASN preparation used, crude cytosolic extract versus affinity-purified recombinant FASN.

Importantly, calculating the specific activity of FASN in mouse tissues based on the immunoblotting quantification of FASN made it possible to discern whether factors other than FASN amount influence the enzyme's activity under steady-state conditions. The novel observation that the specific activity of FASN from lactating mammary epithelial cells is significantly higher (1.26-fold, $P = 0.02$) when compared with FASN from liver suggested that FASN activity may be modified in a tissue-specific manner. It is tempting to speculate that the observed increase between the MECs and liver-specific activity of FASN resulted from the presence of mammary-specific factors that complex with FASN. Alternatively, this increase may be due to the presence of tissue-specific fatty acid binding proteins. Binding of de novo synthesized fatty

acids to binding proteins could enhance catalysis by relieving product inhibition of FASN. Alternatively, protein activators of FASN, such as 4′-phosphopantetheine transferase [40], might exist at different amounts in the two tissues, thereby increasing pantetheinyl activation of the mammary gland FASN. In the end, it is clear that this method can be directly applied to assays with recombinant FASN or column-purified FASN or to partially enriched FASN present in a cell or tissue cytosolic lysate.

In conclusion, we have described a new method that evaluates FASN activity based on the detection and quantitative measurement of enzyme product formation—de novo synthesized [$^{13}C_{16}$]palmitate using GC–MS. This method can be applied to tissues from all mammalian species, and it provides the opportunity to directly compare tissue preparations because FASN amounts are determined. FASN-specific activity is reliably measured in tissues under different metabolic conditions or various physiological and diseased states, and [$^{13}C_{16}$]palmitate synthesis can now be precisely measured from crude extracts without complication from unlabeled fatty acids present in the lysates. FASN is generally seen as an indicator of aggressive tumors and poor patient outcome [9,11]; therefore, this assay could be useful to demonstrate a direct link between FASN activity and disease prognosis. Moreover, this method can be used to investigate the effects of FASN modifying proteins, inhibitory peptides, and small molecule inhibitors. Finally, important kinetic information will likely be obtained about FASN catalysis by direct quantitative measurement enzyme product. Sensitive quantification of FASN catalysis will add to the understanding of this complex multicomponent process, which is remarkably contained entirely within the single enzyme fatty acid synthase.

Acknowledgments

The authors thank S. Smith and A. Witkowski (Children's Hospital Oakland Research Institute) for the generosity of their recombinant FASN needed to conduct this research as well as for their thoughtful discussions regarding this work. The authors acknowledge support from the U.S. Department of Defense Breast Cancer Research Program (BC810596 to M.C.R. and BC098051 to E.A.W.), the Colorado Clinical and Translational Sciences Institute (5UL1RR025780 to R.C.M.), a Lipid MAPS Collaborative Grant from the National Institutes of Health (NIH, GM069338 to R.C.M.), and the NIH (PO1-HD38129 to S.M.A.).

References

[1] S.S. Chirala, H. Chang, M. Matzuk, L. Abu-Elheiga, J. Mao, K. Mahon, M. Finegold, S.J. Wakil, Fatty acid synthesis is essential in embryonic development: fatty acid synthase null mutants and most of the heterozygotes die in utero, Proc. Natl. Acad. Sci. USA 100 (2003) 6358–6363.
[2] A. Jayakumar, M.H. Tai, W.Y. Huang, W. al-Feel, M. Hsu, L. Abu-Elheiga, S.S. Chirala, S.J. Wakil, Human fatty acid synthase: Properties and molecular cloning, Proc. Natl. Acad. Sci. USA 92 (1995) 8695–8699.
[3] S. Smith, A. Witkowski, A.K. Joshi, Structural and functional organization of the animal fatty acid synthase, Prog. Lipid Res. 42 (2003) 289–317.
[4] M.C. Rudolph, J. Monks, V. Burns, M. Phistry, R. Marians, M.R. Foote, D.E. Bauman, S.M. Anderson, M.C. Neville, Sterol regulatory element binding protein (Srebf-1) and dietary lipid regulation of fatty acid synthesis in the mammary epithelium, Am. J. Physiol. Endocrinol. Metab. 299 (2010) E918–E927.
[5] S.A. Kliewer, S.S. Sundseth, S.A. Jones, P.J. Brown, G.B. Wisely, C.S. Koble, P. Devchand, W. Wahli, T.M. Willson, J.M. Lenhard, J.M. Lehmann, Fatty acids and eicosanoids regulate gene expression through direct interactions with peroxisome proliferator-activated receptors alpha and gamma, Proc. Natl. Acad. Sci. USA 94 (1997) 4318–4323.
[6] J. Ross, A.M. Najjar, M. Sankaranarayanapillai, W.P. Tong, K. Kaluarachchi, S.M. Ronen, Fatty acid synthase inhibition results in a magnetic resonance-detectable drop in phosphocholine, Mol. Cancer Ther. 7 (2008) 2556–2565.
[7] V. Rioux, P. Legrand, Saturated fatty acids: simple molecular structures with complex cellular functions, Curr. Opin. Clin. Nutr. Metab. Care 10 (2007) 752–758.
[8] H. Cao, K. Gerhold, J.R. Mayers, M.M. Wiest, S.M. Watkins, G.S. Hotamisligil, Identification of a lipokine, a lipid hormone linking adipose tissue to systemic metabolism, Cell 134 (2008) 933–944.
[9] J.A. Menendez, R. Lupu, Fatty acid synthase and the lipogenic phenotype in cancer pathogenesis, Nat. Rev. Cancer 7 (2007) 763–777.
[10] J.A. Menendez, Fine-tuning the lipogenic/lipolytic balance to optimize the metabolic requirements of cancer cell growth: molecular mechanisms and therapeutic perspectives, Biochim. Biophys. Acta 2010 (1801) 381–391.
[11] F.P. Kuhajda, Fatty-acid synthase and human cancer: new perspectives on its role in tumor biology, Nutrition 16 (2000) 202–208.
[12] V.E. Anderson, G.G. Hammes, Stereochemistry of the reactions catalyzed by chicken liver fatty acid synthase, Biochemistry 23 (1984) 2088–2094.
[13] Y. Seyama, T. Kasama, T. Yamakawa, A. Kawaguchi, K. Saito, Origin of hydrogen atoms in the fatty acids synthesized with yeast fatty acid synthetase, J. Biochem. 82 (1977) 1325–1329.
[14] B.L. Horecker, A. Kornberg, The extinction coefficients of the reduced band of pyridine nucleotides, J. Biol. Chem. 175 (1948) 385–390.
[15] C.C. Chung, K. Ohwaki, J.E. Schneeweis, E. Stec, J.P. Varnerin, P.N. Goudreau, A. Chang, J. Cassaday, L. Yang, T. Yamakawa, O. Kornienko, P. Hodder, J. Inglese, M. Ferrer, B. Strulovici, J. Kusunoki, M.R. Tota, T. Takagi, A fluorescence-based thiol quantification assay for ultra-high-throughput screening for inhibitors of coenzyme A production, Assay Drug Dev. Technol. 6 (2008) 361–374.
[16] D. Cerne, I.P. Zitnik, M. Sok, Increased fatty acid synthase activity in non-small cell lung cancer tissue is a weaker predictor of shorter patient survival than increased lipoprotein lipase activity, Arch. Med. Res. 41 (2010) 405–409.
[17] J.M. Soulie, G.J. Sheplock, W.X. Tian, R.Y. Hsu, Transient kinetic studies of fatty acid synthetase: a kinetic self-editing mechanism for the loading of acetyl and malonyl residues and the role of coenzyme A, J. Biol. Chem. 259 (1984) 134–140.
[18] D.A. Roncari, Fatty acid synthase from human liver, Methods Enzymol. 71 (1981) 73–79.
[19] Y. Seyama, A. Kawaguchi, S. Okuda, T. Yamakawa, New assay method for fatty acid synthetase with mass fragmentography, J. Biochem. 84 (1978) 1309–1314.
[20] K. Ohashi, H. Otsuka, Y. Seyama, Assay of fatty acid synthetase by mass fragmentography using [^{13}C]malonyl-CoA, J. Biochem. 97 (1985) 867–875.
[21] S. Zarini, M.A. Gijon, G. Folco, R.C. Murphy, Effect of arachidonic acid reacylation on leukotriene biosynthesis in human neutrophils stimulated with granulocyte-macrophage colony-stimulating factor and formyl-methionyl-leucyl-phenylalanine, J. Biol. Chem. 281 (2006) 10134–10142.
[22] A.K. Joshi, V.S. Rangan, S. Smith, Differential affinity labeling of the two subunits of the homodimeric animal fatty acid synthase allows isolation of heterodimers consisting of subunits that have been independently modified, J. Biol. Chem. 273 (1998) 4937–4943.
[23] M.C. Rudolph, E.A. Wellberg, S.M. Anderson, Adipose-depleted mammary epithelial cells and organoids, J. Mammary Gland Biol. Neoplasia 14 (2009) 381–386.
[24] B.G. Cox, G.G. Hammes, Steady-state kinetic study of fatty acid synthase from chicken liver, Proc. Natl. Acad. Sci. USA 80 (1983) 4233–4237.
[25] S. Smith, S. Abraham, Fatty acid synthetase from lactating rat mammary gland: 3. Dissociation and reassociation, J. Biol. Chem. 246 (1971) 6428–6435.
[26] S. Omura, The antibiotic cerulenin, a novel tool for biochemistry as an inhibitor of fatty acid synthesis, Bacteriol. Rev. 40 (1976) 681–697.
[27] M. Moche, G. Schneider, P. Edwards, K. Dehesh, Y. Lindqvist, Structure of the complex between the antibiotic cerulenin and its target, β-ketoacyl-acyl carrier protein synthase, J. Biol. Chem. 274 (1999) 6031–6034.
[28] R. Bressler, S. Wakil, The study of fatty acid synthesis: IX. The conversion of malonyl coenzyme A to long chain fatty acids, J. Biol. Chem. 236 (1961) 1643–1651.
[29] A.K. Joshi, S. Smith, Construction of a cDNA encoding the multifunctional animal fatty acid synthase and expression in *Spodoptera frugiperda* cells using baculoviral vectors, Biochem. J. 296 (1993) 143–149.
[30] R.C. Murphy, S.J. Gaskell, New applications of mass spectrometry in lipid analysis, J. Biol. Chem. 286 (2011) 25427–25433.
[31] S. Smith, S. Abraham, Fatty acid synthase from lactating rat mammary gland, Methods Enzymol. 35 (1975) 65–74.
[32] N. Singh, S.J. Wakil, J.K. Stoops, On the question of half- or full-site reactivity of animal fatty acid synthetase, J. Biol. Chem. 259 (1984) 3605–3611.
[33] A. Witkowski, A.K. Joshi, S. Smith, Characterization of the β-carbon processing reactions of the mammalian cytosolic fatty acid synthase: role of the central core, Biochemistry 43 (2004) 10458–10466.
[34] E. Agradi, L. Libertini, S. Smith, Specific modification of fatty acid synthetase from lactating rat mammary gland by chymotrypsin and trypsin, Biochem. Biophys. Res. Commun. 68 (1976) 894–900.
[35] L.J. Libertini, S. Smith, Purification and properties of a thioesterase from lactating rat mammary gland which modifies the product specificity of fatty acid synthetase, J. Biol. Chem. 253 (1978) 1393–1401.
[36] J. Naggert, M.L. Narasimhan, L. DeVeaux, H. Cho, Z.I. Randhawa, J.E. Cronan Jr., B.N. Green, S. Smith, Cloning, sequencing, and characterization of *Escherichia coli* thioesterase (part II), J. Biol. Chem. 266 (1991) 11044–11050.
[37] F.P. Kuhajda, K. Jenner, F.D. Wood, R.A. Hennigar, L.B. Jacobs, J.D. Dick, G.R. Pasternack, Fatty acid synthesis: a potential selective target for antineoplastic therapy, Proc. Natl. Acad. Sci. USA 91 (1994) 6379–6383.
[38] P.M. Ahmad, D.S. Feltman, F. Ahmad, Studies on acetyl-CoA carboxylase and fatty acid synthase from rat mammary gland and mammary tumours, Biochem. J. 208 (1982) 443–452.
[39] X. Wang, W.C. Stanley, C.J. Darrow, H. Brunengraber, T. Kasumov, Assay of the activity of malonyl-coenzyme A decarboxylase by gas chromatography–mass spectrometry, Anal. Biochem. 363 (2007) 169–174.
[40] A.K. Joshi, L. Zhang, V.S. Rangan, S. Smith, Cloning, expression, and characterization of a human 4′-phosphopantetheinyl transferase with broad substrate specificity, J. Biol. Chem. 278 (2003) 33142–33149.